DOI: 10.18721/JPM.13102
УДК 536.25

DIRECT NUMERICAL SIMULATION OF THE TURBULENT RAYLEIGH – BÉNARD CONVECTION IN A SLIGHTLY TILTED CYLINDRICAL CONTAINER

S.I. Smirnov, E.M. Smirnov

Peter the Great St. Petersburg Polytechnic University, St. Petersburg, Russian Federation

Results of direct numerical simulation of the turbulent convection in a bottom-heated cylindrical container have been presented. The height-to-diameter ratio was equal to 1.0. The calculations were performed for two media: mercury (Pr = 0.025) and water (Pr = 6.4) at Ra = 10^6 and 10^8 respectively. To suppress possible azimuthal movements of the global vortex (large-scale circulation) developing in the container, its axis was tilted a small angle with respect to the gravity vector. Structure of the time-averaged flow pattern symmetrical with respect to the central vertical plane was analyzed. Peculiarities of vortex structures developing in the corner zones were revealed. Representative profiles of the Reynolds stresses and components of the turbulent heat flux vector were obtained for the central vertical plane.

Keywords: Rayleigh – Bénard convection, tilted container, turbulence, direct numerical simulation, large-scale circulation

Citation: Smirnov S.I., Smirnov E.M., Direct numerical simulation of the turbulent Rayleigh – Bénard convection in a slightly tilted cylindrical container, St. Petersburg Polytechnical State University Journal. Physics and Mathematics. 13 (1) (2020) 13–23. DOI: 10.18721/JPM.13201

ПРЯМОЕ ЧИСЛЕННОЕ МОДЕЛИРОВАНИЕ ТУРБУЛЕНТНОЙ КОНВЕКЦИИ РЭЛЕЯ – БЕНАРА В СЛЕГКА НАКЛОНЕННОМ ЦИЛИНДРИЧЕСКОМ КОНТЕЙНЕРЕ

С.И. Смирнов, Е.М. Смирнов

Санкт-Петербургский политехнический университет Петра Великого,
Санкт-Петербург, Российская Федерация

Представлены результаты прямого численного моделирования турбулентной конвекции в подогреваемом снизу цилиндрическом контейнере с высотой, равной диаметру. Расчеты проведены для двух сред: воды (Pr = 6,4) и ртути (Pr = 0,025), при числах Рэлея 10^8 и 10^6 соответственно. Ось контейнера наклонена на небольшой угол по отношению к вектору гравитационного ускорения с целью подавления возможных азимутальных перемещений глобального вихря, развивающегося в контейнере. Анализируется структура осредненного конвективного движения, симметричного относительно центрального вертикального сечения. Выявлены особенности вихревого течения в угловых областях, присущие двум рассмотренным случаям. Получены представительные профили всех ненулевых составляющих тензора рейнольдсовых напряжений и вектора турбулентного теплового потока в центральном сечении.

Ключевые слова: конвекция Рэлея – Бенара, наклоненный контейнер, турбулентность, прямое численное моделирование, крупномасштабная циркуляция

Ссылка при цитировании: Смирнов С.И., Смирнов Е.М. Прямое численное моделирование турбулентной конвекции Рэлея – Бенара в слегка наклоненном цилиндрическом контейнере // Научно-технические ведомости СПбГПУ. Физико-математические науки. 2020. Т. 13. № 1. С. 14–25 DOI: 10.18721/JPM.13201

Introduction

There is much interest in study of natural convection, as it is a phenomenon widely found in nature and technologies. Rayleigh–Bénard convection of fluid in a vertically oriented circular cylindrical container is one of the most attractive model problems in this field.

Diverse experimental and numerical studies found that large-scale circulation (LSC) is a characteristic feature of natural convective flow in a cylindrical container heated from below (see, for example, review [1]). If the height of the container is equal to its diameter or close to it, the LSC is a large-scale vortex covering the entire region of convective flow [1–5]. If the container axis is strictly vertical and axisymmetric boundary conditions are imposed, the problem does not have a preferential azimuthal position, and it is reasonable to assume that the global vortex can occasionally move in the azimuthal direction. Experimental studies on Rayleigh–Bénard convection in a circular cylindrical container confirm this, observing slow (ultra-low frequency) changes in LSC orientation, with irregular behavior (see, for example, [3–9]). Liquid metals [3, 4, 9] and water [5–8] are mainly used for experimental studies. Evidently, the azimuthal behavior of LSC is governed in each case by very small, difficult-to-control deviations from axial symmetry, typical for laboratory models. This feature of LSC was also observed in multiple numerical experiments on transitional and turbulent regimes of Rayleigh–Bénard convection in cylindrical containers at Prandtl numbers (Pr) characteristic for liquid metals [10–13], water [11] and air [14–16].

Random changes in azimuthal orientation of LSC are not the only feature of a global vortex structure of this type. It was found that LSC exhibits two more types of oscillations, *sloshing* and *torsional*. In addition, LSC can disappear for relatively short periods of time and reappear with a pronounced reorientation (this is known as cessation). These features of LSC were studied experimentally in [16–20]. *Sloshing* and *torsional* oscillations are also reproduced in numerical solutions (see, for example, the recent study [21] and references therein).

Azimuthal instability of LSC makes it difficult to obtain the statistical characteristics of turbulent convection in cylindrical containers heated from below, including averaged three-dimensional fields of physical quantities describing relatively small-scale background turbulence. LSC can be locked in a certain azimuthal position by introducing a stabilizing external factor that does not considerably alter the intensity and structure of the flow. For example, slightly tilting the container may act as such a factor. This approach has been repeatedly used in experimental studies conducted at different Rayleigh numbers (Ra) for media with Pr = 0.025 [3, 4], 0.7–0.8 [17, 18] and Pr = 4–6 [17, 19, 20, 22–24]. The effects from slight tilt of a container filled with a medium with Pr = 0.025, from non-uniform heating of the horizontal wall and the structure of the computational grid in the central plane were numerically studied in [25].

One of the most popular numerical approaches used for describing turbulent natural convection in relatively simple geometrical regions is Direct Numerical Simulation (DNS), resolving all components of turbulent motion (see, for example, [26–34] carried out for media with different Prandtl numbers: Pr = 0.005 [30], 0.02 [26, 30], 0.1–1.0 [26, 27, 29, 32–34] and 6.4 [28, 31]). A notable recent work [32] presented DNS for turbulent Rayleigh–Bénard convection at Pr = 1, Ra = 10^8 in regions with different geometric configurations (including cylindrical), focusing on comparing the predictions of integral heat transfer provided by different software packages.

Our study is dedicated to direct numerical simulation of turbulent convection in a slightly tilted cylindrical container, whose height is equal to its diameter, heated from below. Results were obtained for the Rayleigh number Ra = 10^6 at the Prandtl number Pr = 0.025 and Ra = 10^8 at Pr = 6.4.

Problem statement

We considered turbulent convection of a fluid with constant physical properties in the Boussinesq approximation for a circular cylindrical container heated from below with a 1:1

height-to-diameter ratio of the cylinder ($\Gamma = D/H = 1$). The container was tilted by a small angle, $\varphi = 2\epsilon$, with respect to the gravity vector (Fig. 1, *a*).

Unsteady fluid motion is described by the following system of equations (1)–(3), including the continuity equation, the Navier–Stokes equations and the convection-diffusion equation.

$$\nabla \cdot \mathbf{V} = 0, \tag{1}$$

$$\frac{\partial \mathbf{V}}{\partial t} + (\mathbf{V} \cdot \nabla)\mathbf{V} = -\frac{1}{\rho}\nabla p + \beta(T_0 - T)\mathbf{g} + \nu\nabla^2\mathbf{V}, \tag{2}$$

$$\frac{\partial T}{\partial t} + (\mathbf{V} \cdot \nabla)T = \chi\nabla^2 T. \tag{3}$$

Here $\mathbf{V} = (V_x, V_y, V_z)$ is the velocity vector in the $x'y'z$ coordinate system; t is the time; p, T, and ρ are the pressure, temperature, and density of the fluid; β, ν, and χ are the coefficients of its thermal expansion, kinematic viscosity, and thermal diffusivity; $\mathbf{g}$ is the gravity vector pointing in the opposite direction from the axis y' and making an angle of 2° with it; T_0 is the fluid temperature under hydrostatic equilibrium.

The solution to system (1)–(3) is obtained in the $x'y'z$ coordinate system, whose axis y' coincides with the axis of the container (see Fig. 1, *a*).

No-flow and no-slip conditions are imposed on all boundaries. Constant temperatures are given for the horizontal walls; it is assumed that the temperature of the top wall (T_c) is lower than the bottom (T_h). The side wall is assumed to be adiabatic.

The dimensionless governing parameters of the problem are the Prandtl number $\mathrm{Pr} = \nu/\chi$ and the Rayleigh number, related as

$$\mathrm{Ra} = \mathrm{Pr}\cdot(V_b H/\nu)^2,$$

where V_b is the characteristic (large-scale) flow velocity (buoyant velocity),

$$V_b = (g\beta\Delta T H)^{0.5}$$

(ΔT is the characteristic temperature difference between the hot (T_h) and the cold (T_c) wall),

$$\Delta T = T_h - T_c.$$

Let us also introduce the Grashof number $\mathrm{Gr} = \mathrm{Ra}/\mathrm{Pr}$, whose square root acts as the equivalent of the Reynolds number in natural convection problems.

The computations below were performed for $\mathrm{Pr} = 0.025$, $\mathrm{Ra} = 10^6$ and $\mathrm{Pr} = 6.4$, $\mathrm{Ra} = 10^8$. The Grashof numbers for these two cases are of the same order and equal $4.0\cdot10^7$ and $1.6\cdot10^7$, respectively.

Computational aspects

The computations were carried out using one of the latest versions of the in-house finite-volume code SINF/Flag-S developed at Peter the Great Polytechnic University (the computational algorithms implemented in the code run on unstructured grids). We used a variation of the fractional step method described in [35]. The Crank–Nicolson scheme with second-order accuracy was used for advancing in time. A central difference scheme was used to approximate the convection and diffusion terms in the continuity equations. The computational grid consisted of approximately

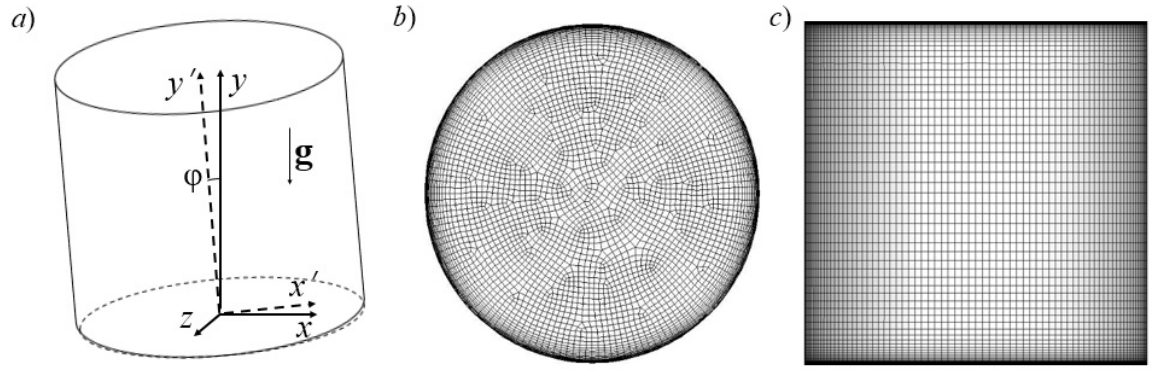

Fig. 1. Geometry of computational domain for tilted container (*a*), grid structure in central horizontal (*b*) and vertical (*c*) planes

$1.5 \cdot 10^7$ hexagonal elements; the grid structure in horizontal and vertical planes is shown in Fig. 1, *b*, *c*. The grid is refined near the walls, while the size of the first near-wall cell was about 10^{-4} *H*. A characteristic feature of the computational grid was a central unstructured (asymmetric) region with a diameter of about 0.8*D* (see Fig. 1, *b*).

The finite-volume computations of Rayleigh–Bénard convection on this grid can be interpreted as direct numerical simulation of turbulence if the local cell size is sufficiently small compared to the size of the smallest vortices in the given region. It is well known the Kolmogorov scale is the smallest scale of turbulent flow if the temperature layers are thicker than the velocity layers (Pr < 1):

$$\delta_K = (\nu^3/\varepsilon)^{0.25},$$

where ε is the dissipation rate of turbulent kinetic energy,

$$\varepsilon = \nu \overline{\frac{\partial V_i'}{\partial x_j} \cdot \frac{\partial V_i'}{\partial x_j}}$$

(V_i' is the fluctuation of the *i*th velocity component, x_j are the Cartesian coordinates).

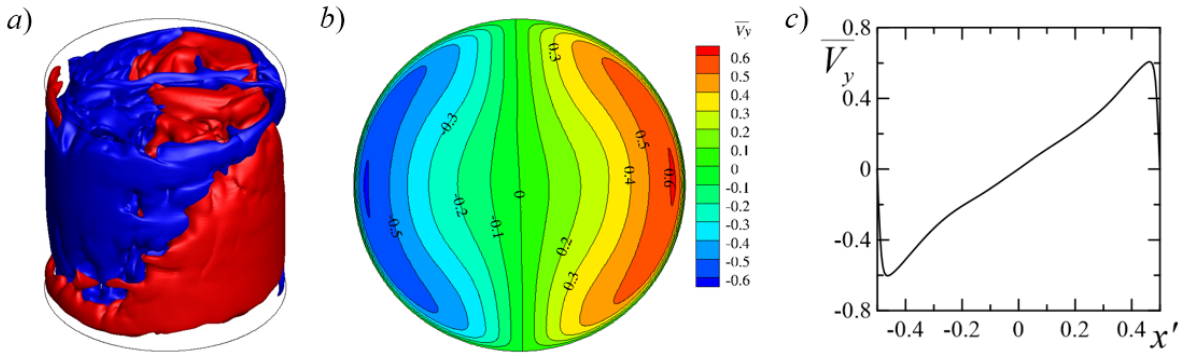

Fig. 2. Distributions of instantaneous (*a*) and averaged (*b*, *c*) vertical velocity components for mercury convection in cylindrical container (CC) heated from below at Pr = 0.025: isosurface components *a*, $|V_y| = 0.14$; distribution *b* in central plane perpendicular to CC axis, $y' = 0.5$; distribution *c* along a line lying in ($x'Oy'$) plane of CC at a height of $y' = 0.5$.
Blue structures correspond to downward flow, red to upward flow.

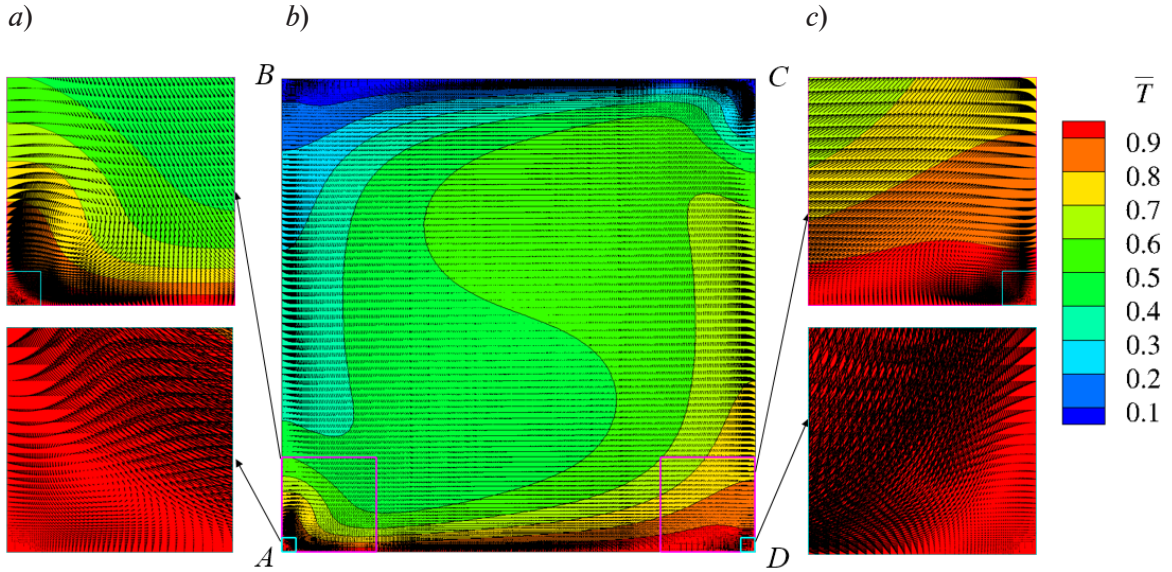

Fig. 3. Averaged temperature field in central vertical plane of container (coinciding with LSC midplane) with superimposed vectors of averaged velocity at Pr = 0.025:
entire convection region of mercury *b*, regions *a*, *c* with corner vortices

If Pr > 1, the smallest scale is the Batchelor scale:

$$\delta_B = \delta_K/\mathrm{Pr}^{0.5}.$$

Accordingly, the quality of the computations can be assessed by comparing the characteristic sizes of the grid elements with different smallest turbulence scales.

The computations started from the zero velocity field and the uniform temperature field, assumed to be equal to $(T_h + T_c)/2$. The time step did not exceed one thousandth of the characteristic time $t_b = H/V_b$, guaranteeing that the local values of the Courant number were less than unity. The computed fields were averaged over time starting after a transient process that lasted about $200t_b$. The samples for averaging were $3000t_b$ for convection of mercury and $4000t_b$ for water.

Computational results and discussion

The quantities **V** and T in the discussion below refer to the velocity and the temperature difference $T - T_c$, related to the corresponding scale (V_b and ΔT), and (x', y', z) refer to the coordinates related to the height of the container.

The quality of grid resolution was assessed after the computations, using the statistics accumulated for the TKE dissipation field. We actually analyzed the fields of the smallest turbulence scales δ_K and δ_B, computed by the above relations and taken relative to the cubic root of the computational cell volume ($V^{1/3}$). It was found that the ratios $\delta_K/V^{1/3}$ and $\delta_B/V^{1/3}$ took values exceeding unity in almost the entire region of the flow. The exceptions were a small area near the side wall, in the layer with the average height, and also the region with the corner vortices, where the smallest values of the ratios $\delta_K/V^{1/3}$ and $\delta_B/V^{1/3}$ were 0.6–0.7.

Results for mercury. Fig. 2, *a* shows an instantaneous distribution for convection of mercury in the cylindrical container heated from below, with pronounced large-scale circulation. Fig. 2, *b*, *c* shows the distribution of the averaged vertical velocity component in the central plane perpendicular to the container axis; the vertical velocity component here and below refers to the velocity component along the axis of a slightly tilted container. Evidently, this distribution has double symmetry, as expected for the case of LSC 'locked' in a certain azimuthal position.

It is of particular interest to explore the characteristic features of convective flow in the central vertical plane of the container, which coincides with the midplane of the LSC (see Fig. 2); this plane is also the $x'Oy'$ plane of the container axis tilt.

ig. 3 shows the vortex structure of the flow and the temperature field in this plane. Notably, aside from LSC, the flow contains several smaller vortices located in the corners of the container. The region occupied by additional

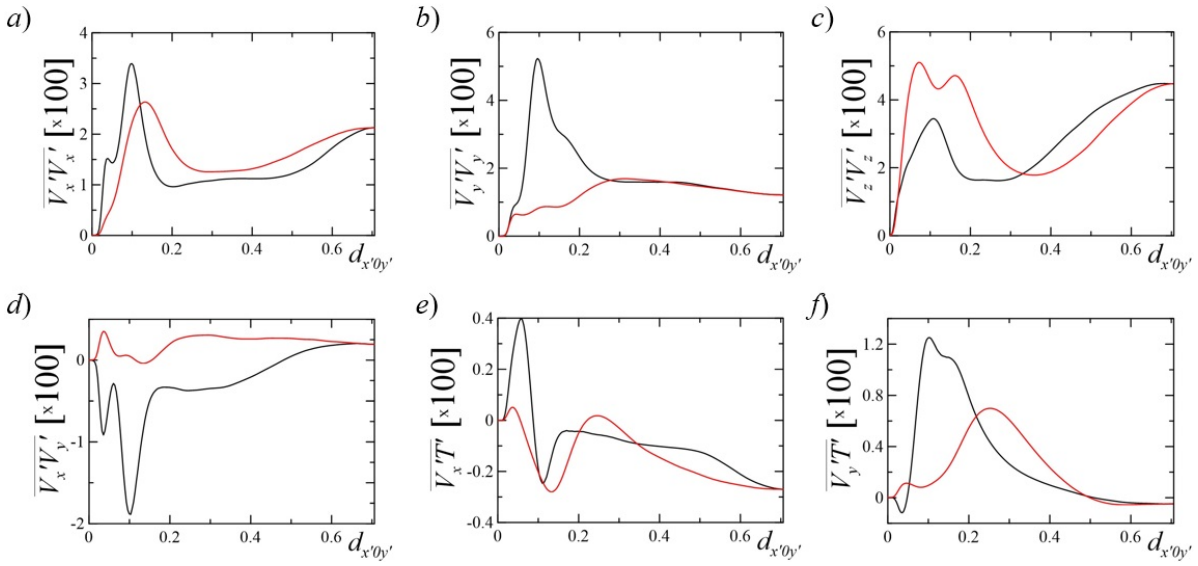

Fig. 4. Distributions of normalized components of Reynolds stress tensor and turbulent heat flux vector along AC (black curve) and BD (red curve) diagonals of container's central plane in case of mercury convection (see Fig. 3), coordinate $d_{x'Oy'} = 0$ at points A and B, respectively

vortices is considerably larger in the corners *A* and *C* (see Fig. 3, *a*) than in the corners *B* and *D* (see Fig. 3, *c*); the intensity of the vortices also differs: it is much higher in the corners *A* and *C*. Gradient layers near the isothermal walls are clearly visible in the temperature field.

We also obtained three-dimensional fields of all components of the Reynolds stress tensor and the turbulent heat flux vector. These data are interesting, in particular, for assessing the capabilities of different second-order turbulence models (Reynolds stress models) used for computations of convective flows based on the Reynolds-averaged Navier–Stokes equations. Data for the central vertical plane of the container are given in this paper. Two of the six components of the Reynolds stress tensor, as well as one of the three components of the turbulent heat flux are equal to zero in this plane due to statistical symmetry of convection.

The distributions of the components of the Reynolds stress tensor and the turbulent heat flux vector are given in Fig. 4 along the diagonals of the central vertical plane (the corresponding coordinate, denoted as $d_{x'Oy'}$, is used). Because the averaged flow is symmetric, distributions are given only for half of the diagonal. Moreover, the given distributions were obtained by averaging over two halves of each of the diagonals (evidently, this technique effectively increases the initial sample for obtaining statistics). Fig. 4 shows that almost all of the given the correlations are close to zero in a small corner region (conditionally, at $d_{x'Oy'} < 0.02$)

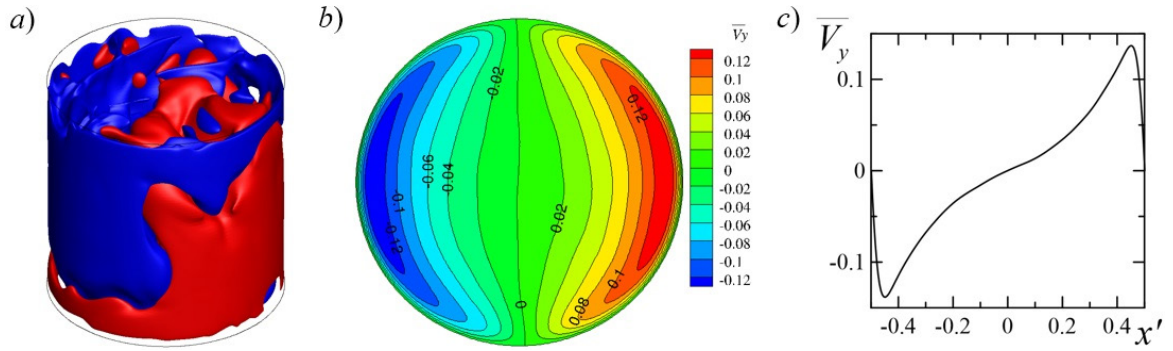

Fig. 5. Distributions of instantaneous (*a*) and averaged (*b*, *c*) vertical velocity components for convection of water in cylindrical container heated from below at Pr = 6.4
The distributions are similar to those shown in Fig. 2 for mercury

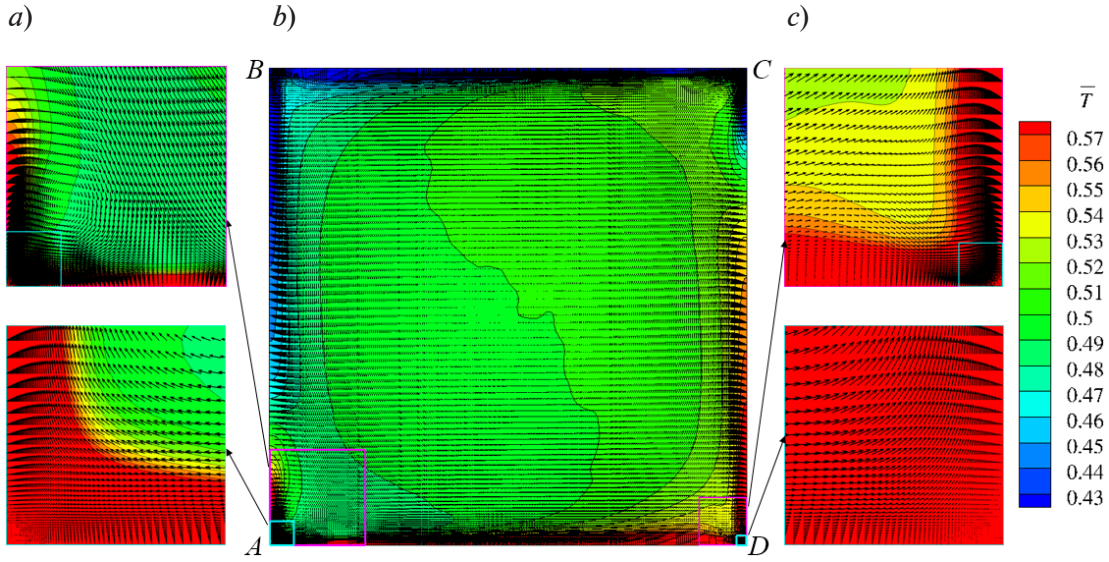

Fig. 6. Averaged temperature field with superimposed vectors of averaged velocity in central vertical plane of container at Pr = 6.4
The distributions are similar to those shown in Fig. 3 for mercury

where there is practically no flow in the medium, with the exception of the Reynolds stress due to fluctuations of the velocity component normal to this plane (see Fig. 4, *c*). With $d_{x'Oy'} > 0.02$, all correlations increase in absolute value to a certain degree, and their variation is essentially nonmonotonic with a further increase in the distance from the corner. This is generally consistent with the picture of the vector velocity field shown in Fig. 3: here, the stable region in the corner is followed by the region where two vortex structures coexist; their presence and interaction determine the nonmonotonic behavior of the distributions shown in Fig. 4. The spans of nonmonotonic segments are somewhat different depending on the choice of the diagonal (AC or *BD*). The region covered by LSC follows the zones occupied by corner vortices ($d_{x'Oy'} > 0.15...0.2$); the correlations change relatively smoothly within this region.

The integral value of the Nusselt number for convection of mercury, obtained as a result of these computations with $\mathrm{Ra} = 10^6$, was $\mathrm{Nu} = 5.64$, which is in good agreement with the results of previous studies carried out in the framework of the implicit LES (ILES) approach: $\mathrm{Nu} = 5.70$ [25], $\mathrm{Nu} = 5.58$ [35], and also with the DNS results, $\mathrm{Nu} = 5.43$ [30].

Results for water. Similar distributions are shown in Figs. 5–7 for convection of water ($\mathrm{Pr} = 6.4$) at $\mathrm{Ra} = 10^8$.

We can conclude from the distributions of the averaged vertical velocity and temperature (Fig. 5) that the solution obtained is also symmetric with respect to the LSC midplane (central vertical plane) in this case. In case of long samples, symmetric statistical characteristics of the flow can be obtained only if the LSC is 'locked' in a certain azimuthal position. Comparing the computational data shown in Figs. 2 and 5, we can establish that the maximum values of the normalized vertical velocity for convection of water are lower than for convection of mercury by approximately five times.

Fig. 6 shows the structure of convective flow of water in the central vertical plane. The same as in in the case of mercury convection considered above (Fig. 3), large-scale circulation of water is complemented by corner vortex structures. However, unlike convection of mercury, there is only one pronounced vortex in each of the corners *A* and *C*, and there are no intense vortices at all in the corners *B* and *D*; the flow turns sharply here, and a small region with very slow motion evolves. These characteristics of water convection in a cylindrical container were earlier discussed in [15]. As expected, high-gradient layers form in the temperature field near the isothermal walls.

Fig. 7 shows the distributions of the nonzero components of the Reynolds stress tensor and the turbulent heat flux vector along the diagonals of the central vertical plane. In

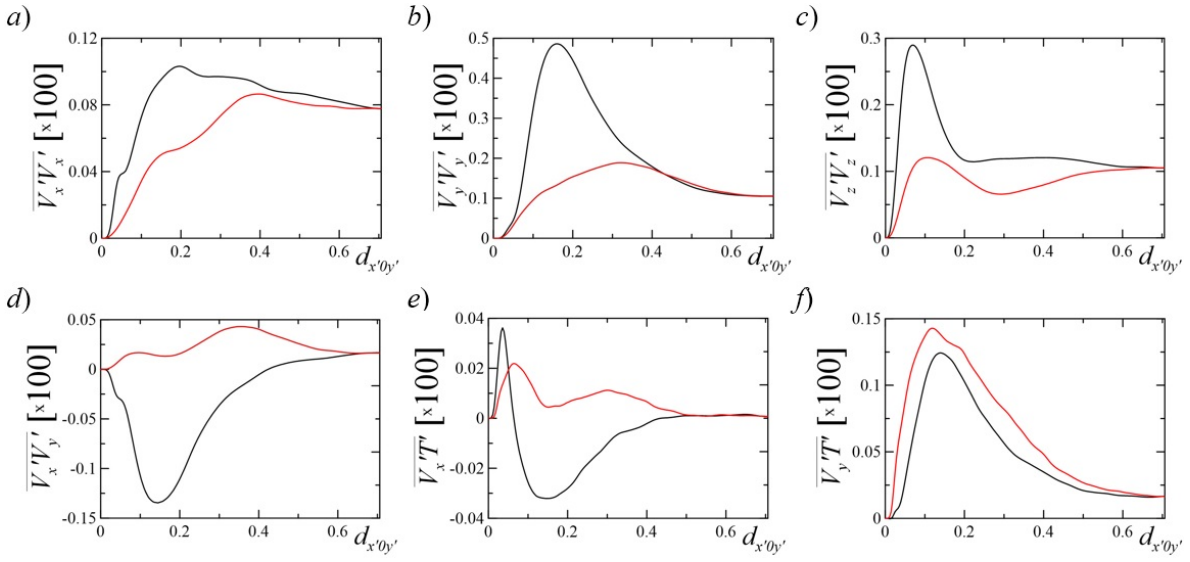

Fig. 7. Distributions of normalized components of Reynolds stress tensor and turbulent heat flux vector along *AC* (black curve) and *BD* (red curve) diagonals of central vertical plane of container for water convection (see Fig. 6), coordinate $d_{x'Oy'} = 0$ at points *A* and *B*, respectively

contrast to convection of mercury, the correlations given for Pr = 6.4 generally change more smoothly; evidently, this is because the corner vortex structures are underdeveloped in case of convection of a fluid with a large Prandtl number. However, segments where the effect of corner vortices can be observed are also visible in this case in the given distributions. Furthermore, compared with the previous case (see Fig. 4), the general level of normalized correlations characterizing the intensity of turbulent transfer is less by about 1 to 1.5 orders of magnitude for convection of water than for a fluid with a small Prandtl number.

The integral Nusselt number obtained for convection of water with $Ra = 10^8$ was Nu = 33.0, which coincides with the results of previous computations [28] performed using the DNS method up to three significant digits.

Conclusion

Direct numerical simulation helped accumulate a large amount of statistical data for essentially three-dimensional turbulent convection in a slightly tilted cylindrical container heated from below, whose height equals the diameter. Computations were carried out for $Ra = 10^6$ at Pr = 0.025 (mercury), and for $Ra = 10^8$ at Pr = 6.4 (water).

We have found that tilting the container axis by 2° relative to the gravity vector allows to reliably 'lock' the global vortex (large-scale circulation (LSC)) in a certain azimuthal position.

The pattern of the averaged flow in the central vertical plane of the container, coinciding with the midplane of the LSC, is characterized by a combination of LSC with corner vortex structures, which are most pronounced for convection of the medium with a small Prandtl number.

We have computed three-dimensional fields of all components of the Reynolds stress tensor and the turbulent heat flux vector. These data can serve, in particular, for assessing the capabilities of different second-order turbulence models (Reynolds stress models) used to compute convective flows based on the Reynolds-averaged Navier–Stokes equations.

The values obtained for the Nusselt integral number are in good agreement with the data given in literature for a container with a vertical axis.

This study was supported by the Russian Foundation for Basic Research (Grant for Vortex-Resolving Numerical Modeling of Turbulent Natural Convection under Conjugate Heat Transfer Conditions no. 17-08-01543).

The computational data were obtained using the resources of the Supercomputer Center at Peter the Great Polytechnic University (www.scc.spbstu.ru).

REFERENCES

1. **Ahlers G., Grossmann S., Lohse D.**, Heat transfer and large scale dynamics in turbulent Rayleigh-Bénard convection, Rev. Mod. Phys. 81 (2) (2009) 503–538.

2. **Takeshita T., Segawa T., Glazier J.A., Sano M.,** Thermal turbulence in mercury, Phys. Rev. Lett. 76 (9) (1996) 1465–1468.

3. **Cioni S., Ciliberto S., Sommeria J.,** Experimental study of high-Rayleigh-number convection in mercury and water, Dyn. Atmos. Oceans. 24 (1) (1996) 117–127.

4. **Cioni S., Ciliberto S., Sommeria J.,** Strongly turbulent Rayleigh–Bénard convection in mercury: comparison with results at moderate Prandtl number, J. Fluid Mech. 335 (1) (1997) 111–140.

5. **Qui X.-L., Tong P.,** Large-scale velocity structures in turbulent thermal convection, Phys. Rev. E. 64 (3) (2001) 036304.

6. **Niemela J.J., Skrbek L., Sreenivasan K.R., Donnelly R.J.,** The wind in confined thermal convection, J. Fluid Mech. 449 (2001) (25 December) 169–178.

7. **Sreenivasan K.R., Bershadskii A., Niemela J.J.,** Mean wind and its reversal in thermal convection, Phys. Rev. E. 65 (5) (2002) 056306.

8. **Brown E., Nikolaenko A., Ahlers G.,** Reorientation of the large-scale circulation in turbulent Rayleigh–Bénard convection, Phys. Rev. Lett. 95 (8) (2005) 084503.

9. **Khalilov R., Kolesnichenko I., Pavlinov A., et al.,** Thermal convection of liquid sodium in inclined cylinders, Phys. Rev. Fluids. 3 (4) (2018) 043503.

10. **Verzicco R., Camussi R.,** Transitional regimes of low-Prandtl thermal convection in a cylindrical cell, Phys. Fluids. 9 (5) (1997) 1287–1295.

11. **Abramov A.G., Ivanov N.G., Smirnov E.M.,** Numerical study of high-Ra Rayleigh–Bénard mercury and water convection in confined enclosures using a hybrid RANS/LES technique, Proc. of the Eurotherm Seminar 74, Eindhoven, TUE. (2003) 33–38.

12. **Schumacher J., Bandaru V., Pandey A., Scheel J.D.,** Transitional boundary layers in low-Prandtl-number convection, Phys. Rev. Fluids. 1 (8) (2016) 084402.

13. **Smirnov S.I., Smirnovsky A.A.,** Numerical simulation of turbulent mercury natural convection in a heated-from-below cylinder with zero and non-zero thickness of the horizontal walls, Thermal Processes in Engineering. 10 (3–4) (2018) 94–100 (in Russian).

14. **Benzi R., Verzicco R.,** Numerical simulations of flow reversal in Rayleigh–Bénard convection, Europhysics Letters. 81 (6) (2008) 64008.

15. **Wagner S., Shishkina O., Wagner C.,** Boundary layers and wind in cylindrical Rayleigh–Bénard cells, J. Fluid Mech. 697 (2012) (25 April) 336–366.

16. **Mishra P.K., De A.K., Verma M.K., Eswaran V.,** Dynamics of reorientations and reversals of large-scale flow in Rayleigh–Bénard convection, J. Fluid Mech. 668 (10 February) (2011) 480–499.

17. **Roche P.-E., Gauthier F., Kaiser R., Salort J.,** On the triggering of the ultimate regime of convection, New J. Phys. 12 (8) (2010) 085014.

18. **He X., van Gils D.P.M., Bodenschatz E., Ahlers G.,** Reynolds numbers and the elliptic approximation near the ultimate state of turbulent Rayleigh–Bénard convection, New J. Phys. 17 (6) (2015) 063028.

19. **Chilla F., Rastello M., Chaumat S., Castaing B.,** Long relaxation times and tilt sensitivity in Rayleigh–Bénard turbulence, Eur. Phys. J. B. 40 (2) (2004) 223–227.

20. **Ahlers G., Brown E., Nikolaenko A.,** The search for slow transients, and the effect of imperfect vertical alignment, in turbulent Rayleigh–Bénard convection, J. Fluid Mech. 557 (25 June) (2006) 347–367.

21. **Zwirner L., Khalilov R., Kolesnichenko I., et al.,** The influence of the cell inclination on the heat transport and large-scale circulation in liquid metal convection, J. Fluid Mech. 884 (10 February) (2020) A18.

22. **Brown E., Ahlers G.,** The origin of oscillations of the large-scale circulation of turbulent Rayleigh–Bénard convection, J. Fluid Mech. 638 (10 November) (2009) 383–400.

23. **Xi H.-D., Zhou S.-Q., Zhou Q., et al.,** Origin of the temperature oscillation in turbulent thermal convection, Phys. Rev. Lett. 102 (4) (2009) 044503.

24. **Weiss S., Ahlers G.,** Effect of tilting on turbulent convection: cylindrical samples with aspect ratio $\Gamma = 0.50$, J. Fluid Mech. 715 (25 January) (2013) 314–334.

25. **Smirnov S.I., Abramov A.G., Smirnov E.M.,** Numerical simulation of turbulent Rayleigh–Bénard mercury convection in a circular cylinder with introducing small deviations from the axisymmetric formulation, J. Phys.: Conf. Ser. 1359 (2019) 012077.

26. **Van der Poel E.P., Stevens R.J.A.M., Lohse D.,** Comparison between two- and three-dimensional Rayleigh–Bénard convection, J. Fluid Mech. 736 (10 December) (2013) 177–194.

27. **Scheel J.D., Schumacher J.,** Local boundary layer scales in turbulent Rayleigh–Bénard convection, J. Fluid Mech. 758 (10 November) (2014) 344–373.

28. **Kooij G.L., Botchev M.A., Geurts B.J.,** Direct numerical simulation of Nusselt number scaling in rotating Rayleigh–Bénard convection, Int. J. Heat Fluid Flow. 55 (October) (2015) 26–33.

29. **Horn S., Shishkina O.,** Toroidal and poloidal energy in rotating Rayleigh–Bénard convection, J. Fluid Mech. 762 (10 January) (2015) 232–255.

30. **Scheel J.D., Schumacher J.,** Global and local statistics in turbulent convection at low Prandtl numbers, J. Fluid Mech. 802 (10 September) (2016) 147–173.

31. **Sakievich P.J., Peet Y.T., Adrian R.J.,** Large-scale thermal motions of turbulent Rayleigh–Bénard convection in a wide aspect-ratio cylindrical domain, Int. J. Heat Fluid Flow. 61 A (October) (2016) 193–196.

32. **Kooij G.L., Botchev M.A., Frederix E.M.A., et al.,** Comparison of computational codes for direct numerical simulations of turbulent Rayleigh–Bénard convection, Computers & Fluids. 166 (30 April) (2018) 1–8.

33. **Zwirner L., Shishkina O.,** Confined inclined thermal convection in low-Prandtl-number fluids, J. Fluid Mech. 850 (10 September) (2018) 984–1008.

34. **Wan Z.-H., Wei P., Verzicco R., et al.,** Effect of sidewall on heat transfer and flow structure in Rayleigh–Bénard convection, J. Fluid Mech. 881 (25 December) (2019) 218–243.

35. **Smirnov S.I., Smirnov E.M., Smirnovsky A.A.,** Endwall heat transfer effects on the turbulent mercury convection in a rotating cylinder, St. Petersburg Polytechnical University Journal. Physics and Mathematics. 3 (2) (2017) 83–94.

Received 20.01.2020, accepted 12.02.2020.

THE AUTHORS

SMIRNOV Sergei I.
Peter the Great St. Petersburg Polytechnic University
29 Politechnicheskaya St., St. Petersburg, 195251, Russian Federation
sergeysmirnov92@mail.ru

SMIRNOV Evgueni M.
Peter the Great St. Petersburg Polytechnic University
29 Politechnicheskaya St., St. Petersburg, 195251, Russian Federation
smirnov_em@spbstu.ru

СПИСОК ЛИТЕРАТУРЫ

1. **Ahlers G., Grossmann S., Lohse D.** Heat transfer and large scale dynamics in turbulent Rayleigh–Bénard convection // Rev. Mod. Phys. 2009. Vol. 81. No. 2. Pp. 503–538.

2. **Takeshita T., Segawa T., Glazier J.A., Sano M.** Thermal turbulence in mercury // Phys. Rev. Lett. 1996. Vol. 76. No. 9. Pp. 1465–1468.

3. **Cioni S., Ciliberto S., Sommeria J.** Experimental study of high-Rayleigh-number convection in mercury and water // Dyn. Atmos. Oceans. 1996. Vol. 24. No. 1. Pp. 117–127.

4. **Cioni S., Ciliberto S., Sommeria J.** Strongly turbulent Rayleigh–Bénard convection in mercury: comparison with results at moderate Prandtl number // J. Fluid Mech. 1997. Vol. 335. No. 1. Pp. 111–140.

5. **Qui X.-L., Tong P.** Large-scale velocity structures in turbulent thermal convection // Phys. Rev. E. 2001. Vol. 64. No. 3. P. 036304.

6. **Niemela J.J., Skrbek L., Sreenivasan K.R., Donnelly R.J.** The wind in confined thermal convection // J. Fluid Mech. 2001. Vol. 449. 25 December. Pp. 169–178.

7. **Sreenivasan K.R., Bershadskii A., Niemela J.J.** Mean wind and its reversal in thermal convection // Phys. Rev. E. 2002. Vol. 65. No. 5. P. 056306.

8. **Brown E., Nikolaenko A., Ahlers G.** Reorientation of the large-scale circulation in turbulent Rayleigh–Bénard convection // Phys. Rev. Lett. 2005. Vol. 95. No. 8. P. 084503.

9. **Khalilov R., Kolesnichenko I., Pavlinov A., Mamykin A., Shestakov A., Frick P.** Thermal convection of liquid sodium in inclined cylinders // Phys. Rev. Fluids. 2018. Vol. 3. No. 4. P. 043503.

10. **Verzicco R., Camussi R.** Transitional regimes of low-Prandtl thermal convection in a cylindrical cell // Phys. Fluids. 1997. Vol. 9. No. 5. Pp. 1287–1295.

11. **Abramov A.G., Ivanov N.G., Smirnov E.M.** Numerical study of high-Ra Rayleigh-Bénard mercury and water convection in confined enclosures using a hybrid RANS/LES technique // Proc. of the Eurotherm Seminar 74. Eindhoven, TUE, 2003. Pp. 33–38.

12. **Schumacher J., Bandaru V., Pandey A., Scheel J.D.** Transitional boundary layers in low-Prandtl-number convection // Phys. Rev. Fluids. 2016. Vol. 1. No. 8. P. 084402.

13. **Смирнов С.И., Смирновский А.А.** Численное моделирование турбулентной свободной конвекции ртути в подогреваемом снизу цилиндре при нулевой и конечной толщине горизонтальных стенок // Тепловые процессы в технике. 2018. Т. 10. № 3–4. С. 94–100.

14. **Benzi R., Verzicco R.** Numerical simulations of flow reversal in Rayleigh–Bénard convection // Europhysics Letters. 2008. Vol. 81. No. 6. P. 64008.

15. **Wagner S., Shishkina O., Wagner C.** Boundary layers and wind in cylindrical Rayleigh–Bénard cells // J. Fluid Mech. 2012. Vol. 697. 25 April. Pp. 336–366.

16. **Mishra P.K., De A.K., Verma M.K., Eswaran V.** Dynamics of reorientations and reversals of large-scale flow in Rayleigh–Bénard convection // J. Fluid Mech. 2011. Vol. 668. 10 February. Pp. 480–499.

17. **Roche P.-E., Gauthier F., Kaiser R., Salort J.** On the triggering of the Ultimate Regime of convection // New J. Phys. 2010. Vol. 12. No. 8. P. 085014.

18. **He X., van Gils D.P.M., Bodenschatz E., Ahlers G.** Reynolds numbers and the elliptic approximation near the ultimate state of turbulent Rayleigh–Bénard convection // New J. Phys. 2015. Vol. 17. No. 6. P. 063028.

19. **Chilla F., Rastello M., Chaumat S., Castaing B.** Long relaxation times and tilt sensitivity in Rayleigh–Bénard turbulence // Eur. Phys. J. B. 2004. Vol. 40. No. 2. Pp. 223–227.

20. **Ahlers G., Brown E., Nikolaenko A.** The search for slow transients, and the effect of imperfect vertical alignment, in turbulent Rayleigh–Bénard convection // J. Fluid Mech. 2006. Vol. 557. 25 June. Pp. 347–367.

21. **Zwirner L., Khalilov R., Kolesnichenko I., Mamykin A., Mandrykin S., Pavlinov A., Shestakov A., Teimurazov A., Frick P., Shishkina O.** The influence of the cell inclination on the heat transport and large-scale circulation in liquid metal convection // J. Fluid Mech. 2020. Vol. 884. 10 February. P. A18.

22. **Brown E., Ahlers G.** The origin of oscillations of the large-scale circulation of turbulent Rayleigh–Bénard convection // J. Fluid Mech. 2009. Vol. 638. 10 November. Pp. 383–400.

23. **Xi H.-D., Zhou S.-Q., Zhou Q., Chan T.S., Xia K.-Q.** Origin of the temperature oscillation in turbulent thermal convection // Phys. Rev. Lett. 2009. Vol. 102. No. 4. P. 044503.

24. **Weiss S., Ahlers G.** Effect of tilting on turbulent convection: cylindrical samples with aspect ratio $\Gamma = 0.50$ // J. Fluid Mech. 2013. Vol. 715. 25 January. Pp. 314–334.

25. **Smirnov S.I., Abramov A.G., Smirnov E.M.** Numerical simulation of turbulent Rayleigh–Bénard mercury convection in a circular cylinder with introducing small deviations from the axisymmetric formulation // J. Phys.: Conf. Ser. 2019. Vol. 1359. 15–22 September, Yalta, Crimea. P. 012077.

26. **Van der Poel E.P., Stevens R.J.A.M., Lohse D.** Comparison between two- and three-dimensional Rayleigh–Bénard convection // J. Fluid Mech. 2013. Vol. 736. 10 December. Pp. 177–194.

27. **Scheel J.D., Schumacher J.** Local boundary layer scales in turbulent Rayleigh–Bénard convection // J. Fluid Mech. 2014. Vol. 758. 10 November. Pp. 344–373.

28. **Kooij G.L., Botchev M.A., Geurts B.J.** Direct numerical simulation of Nusselt number scaling in rotating Rayleigh–Bénard convection // Int. J. Heat Fluid Flow. 2015. Vol. 55. October. Pp. 26–33.

29. **Horn S., Shishkina O.** Toroidal and poloidal energy in rotating Rayleigh–Bénard convection // J. Fluid Mech. 2015. Vol. 762. 10 January. Pp. 232–255.

30. **Scheel J.D., Schumacher J.** Global and local statistics in turbulent convection at low Prandtl numbers // J. Fluid Mech. 2016. Vol. 802. 10 September. Pp. 147–173.

31. **Sakievich P.J., Peet Y.T., Adrian R.J.** Large-scale thermal motions of turbulent Rayleigh–Bénard convection in a wide aspect-ratio cylindrical domain // Int. J. Heat Fluid Flow. 2016. Vol. 61. Part A. October. Pp. 193–196.

32. **Kooij G.L., Botchev M.A., Frederix E.M.A., Geurts B.J., Horn S., Lohse D., van der Poel E.P., Shishkina O., Stevens R.J.A.M., Verzicco R.** Comparison of computational codes for direct numerical simulations of turbulent Rayleigh–Bénard convection // Computers & Fluids. 2018. Vol. 166. 30 April. Pp. 1–8.

33. **Zwirner L., Shishkina O.** Confined inclined thermal convection in low-Prandtl-number fluids // J. Fluid Mech. 2018. Vol. 850. 10 September. Pp. 984–1008.

34. **Wan Z.-H., Wei P., Verzicco R., Lohse D., Ahlers G., Stevens R.J.A.M.** Effect of sidewall on heat transfer and flow structure in Rayleigh–Bénard convection // J. Fluid Mech. 2019. Vol. 881. 25 December. Pp. 218–243.

35. Смирнов **С.И., Смирнов Е.М., Смирновский А.А.** Влияние теплопереноса в торцевых стенках на турбулентную конвекцию ртути во вращающемся цилиндре // Научно-технические ведомости СПбГПУ. Физико-математические науки. 2017. Т. 10. № 1. С. 31–46.

Статья поступила в редакцию 20.01.2020, принята к публикации 12.02.2020.

СВЕДЕНИЯ ОБ АВТОРАХ

СМИРНОВ Сергей Игоревич – *инженер научно-образовательного центра «Компьютерные технологии в аэродинамике и теплотехнике» Санкт-Петербургского политехнического университета Петра Великого.*

195251, Российская Федерация, г. Санкт-Петербург, Политехническая ул., 29
sergeysmirnov92@mail.ru

СМИРНОВ Евгений Михайлович – *доктор физико-математических наук, профессор Высшей школы прикладной математики и вычислительной физики Санкт-Петербургского политехнического университета Петра Великого.*

195251, Российская Федерация, г. Санкт-Петербург, Политехническая ул., 29
smirnov_em@spbstu.ru